Virchows Arch (1998) 433:173–181

ORIGINAL ARTICLE

Shinichi Yachida · Yasutaka Kokudo
Hisao Wakabayashi · Takashi Maeba · Kenji Kaneda
Hajime Maeta

Morphological and functional alterations to sinusoidal endothelial cells in the early phase of endotoxin-induced liver failure after partial hepatectomy in rats

Received: 8 December 1997 / Accepted: 19 February 1998

Abstract Liver failure following major hepatectomy is characterized pathologically by massive hepatic necrosis, which is thought to begin with injury of sinusoidal endothelial cells (SECs). To examine the early events of SECs leading to hepatic damage, we performed time-course analyses of the morphological and functional perturbation of SECs after endotoxin administration to hepatectomized rats. At 1.5 h after endotoxin injection, when hepatocellular damage was not yet evident, SECs showed augmented expression of intercellular adhesion molecule-1, with frequent adherence of infiltrating leucocytes and ultrastructural features of defenestration and hypertrophied cytoplasm enriched with cell organelles. The serum level of hyaluronate, as an indicator of the functional state of SECs, was significantly elevated. At 3 h, SECs underwent necrosis and disruption, accompanied by fibrin deposits with concomitant hepatocellular necrosis. The morphological and functional alterations of SECs precede necrotic changes in hepatocytes and SECs in endotoxin-induced liver failure after partial hepatectomy.

Key words Sinusoidal endothelial cells · Hyaluronate · Defenestration · Liver failure · Endotoxin

Introduction

The hepatic failure often encountered after extensive surgical resection of the liver has a high morbidity and mortality, despite recent improvements in the care of patients [22]. While the underlying mechanisms are not fully understood, the clinico-pathological state resembles that of sepsis [19]. Recent clinical and experimental studies have demonstrated that bacterial translocation into the mesenteric lymph nodes and liver or endotoxaemia often occurs immediately after major hepatectomy [36, 37] and that the hepatic inflammatory response associated with this event promotes liver failure [4]. These findings suggest the involvement of endotoxin in the pathogenesis of postoperative liver failure.

Low-dose endotoxin administration after two-thirds hepatectomy causes massive hepatic necrosis in rats, resembling human postoperative liver failure [20]. The severe hepatic damage induced in this model is initiated by destruction of sinusoidal endothelial cells (SECs), which is provoked by endotoxin-activated hepatic macrophages [10]. Previous ultrastructural analyses have demonstrated that SEC destruction appears 5 h after endotoxin injection with concomitant injury of hepatocytes [20]. However, there have been no detailed studies on the relationship between morphological changes and functional perturbation of SECs before the manifestation of liver injury.

The serum level of hyaluronate, a major extracellular matrix component, has been used as an indicator of SEC function, because SECs specifically incorporate hyaluronate via binding to receptors and rapidly remove it from the circulation [14]. Since normal SECs have the capacity to eliminate approximately 10 times the normal endogenous amount of hyaluronate, serum hyaluronate levels are not markedly influenced by increased input from the tissue but depend predominantly on the scavenging function of SECs [6, 14]. It has been shown that serum hyaluronate levels are elevated in liver cirrhosis [34] and liver grafts [27], which are accompanied by transformation and destruction, respectively, of SECs.

In order to examine the early morphological and functional events in SECs before the manifestation of hepatic injury in the development of liver failure, we investigated the time-course of light and electron microscopic changes in SECs and serum hyaluronate levels as an indicator of the functional state of SECs in the rat model.

S. Yachida (✉) · Y. Kokudo · H. Wakabayashi · T. Maeba
H. Maeta
First Department of Surgery, Faculty of Medicine,
Kagawa Medical University, 1750–1 Ikenobe, Miki-cho,
Kita-gun, Kagawa 761–0793, Japan
e-mail: surgery1@kms.ac.jp
Tel.: (+81)87-891-2186, Fax: (+81)87-891-2187

K. Kaneda
Department of Anatomy, Osaka City University Medical School,
Osaka, Japan

Materials and methods

Male Sprague-Dawley rats weighing 160–220 g were purchased from CLEA Japan (Tokyo, Japan). They were housed under specific pathogen-free conditions with a 12-h light/dark cycle and at a constant temperature of 24°C, and fed standard chow pellets and water ad libitum. Animals were allowed to acclimatize to our laboratory conditions for 4–6 days before being used for experiments. Experiments were performed in accordance with the standard guidelines for animal experiments at Kagawa Medical University.

In all, 120 rats were used. Under anaesthesia with isoflurane (Abbott Laboratories, North Chicago, Ill.), they were subjected to two-thirds resection of the liver according to the method of Higgins and Anderson [13]. Forty-eight hours later, 200 μg/kg body weight of endotoxin (*Escherichia coli* 0127:B8; Difco Laboratories, Detroit, Mich.) dissolved in saline at a concentration of 250 μg/ml or saline alone (controls) was administered i.v. Then 80 rats were used for the studies reported below and the remaining 40 rats, for the survival study.

For the measurement of intrahepatic blood flow, at 0, 1.5, 3 and 5 h after endotoxin or saline administration the abdomen was opened under isoflurane anaesthesia. The intrahepatic blood flow per unit square of the liver surface was quantitated with a laser-Doppler flowmeter (ALF21 N, Advance, Tokyo, Japan) [2, 24]. Averages of the blood flow in the three unresected lobes (the caudate process, papillary process and right lobe) were generated and expressed as percentages of the values obtained before hepatectomy.

Immediately after the measurement of intrahepatic blood flow, peripheral blood was collected from the inferior vena cava and serum hyaluronate levels were measured with a sandwich binding protein assay system (Chugai Pharmaceutical Co., Tokyo, Japan) [5]. Serum levels of aspartate aminotransferase, alanine aminotransferase and total bilirubin were determined using a Hitachi 7050 automatic analyser (Hitachi, Tokyo, Japan). The determination of tumour necrosis factor-α (TNF-α) in plasma was performed in a 96-well microtiter plate using a TNF-α test kit (Genzyme, Cambridge, Mass.) based on an enzyme-linked immunosorbent assay. All samples were tested in duplicate. The plate was read on a microplate reader MTP-120 (Corona Electric Co., Ibaragi, Japan) at 450 nm. The concentration of TNF-α was calculated from a standard curve.

After perfusion with saline via the portal vein for 1 min, the liver was taken out, immersed in OCT compound (Miles, Elkhart, Ind.) and frozen in liquid nitrogen. Cryosections 5 μm thick were cut on a cryostat (Bright Instrument Co., Huntingdon, UK) and air-dried immediately. Sections were fixed in absolute acetone at 4°C for 10 min, and stained using the labelled streptavidin-biotin method (Dako LSAB Kit, HRP, Dako, Carpinteria, Calif.). Endogenous peroxidase activity was blocked by incubating the sections in methanol containing 0.03% hydrogen peroxide for 5 min at room temperature. Nonspecific staining was blocked by the treatment with 1% bovine serum albumin for 5 min at room temperature. Sections were then incubated with mouse anti-rat intercellular adhesion molecule-1 (ICAM-1) monoclonal antibody (1:1000, Seikagaku, Tokyo, Japan) for 30 min [32], followed by sequential 10-min incubations with biotinylated anti-mouse IgG1 antibody and peroxidase-labelled streptavidin. Reaction products were developed by 3,3′-diaminobenzidine tetrahydrochloride solution containing 0.01% hydrogen peroxide (Dako, Carpinteria, Calif.). Nuclei were counterstained with haematoxylin.

For light and electron microscopy the liver was perfused first with saline via the portal vein with a perfusion pressure of 20 cmH_2O and then with fixative containing 1.5% glutaraldehyde in 0.062 M cacodylate buffer, pH 7.4, plus 1% sucrose or fixative containing 2.5% glutaraldehyde in 0.1 M cacodylate buffer, pH 7.4, for transmission electron microscopy (TEM) or scanning electron microscopy (SEM), respectively. Materials were obtained from several different portions of the caudate process and right lobe, and cut into small pieces of approximately 1 mm^3. They were postfixed in 1% OsO_4 in 0.1 M cacodylate buffer, pH 7.4, at 4°C for 2 h. They were then dehydrated in ethanol series and embedded in polybed (Polyscience, Warrington, Penn.). Sections 0.5 μm thick were cut and stained with toluidine blue and observed by light microscopy (LM). For TEM, thin sections were stained with saturated uranyl acetate and lead citrate and observed in a JEM-1200EX-II electron microscope (JEOL, Tokyo, Japan).

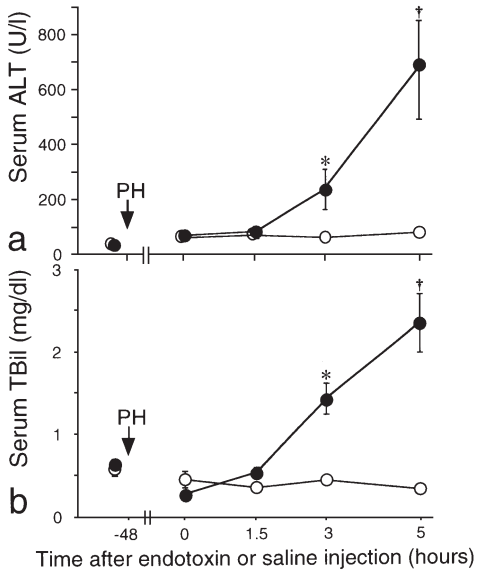

Fig. 1 **a** Serum alanine aminotransferase (ALT) and **b** total bilirubin (TBil) levels before partial hepatectomy (*PH*) and at various time points after i.v. injection of saline (-○-) or 200 μg/kg body weight of endotoxin (-●-). Hepatectomy was performed 48 h before saline or endotoxin administration. Eight rats were examined at each time point. Data are means±standard errors. **P*<0.05, †*P*<0.005 versus the value for saline-treated rats at each time point

For SEM, postfixed materials were freeze-fractured in liquid nitrogen, stained with 2% tannic acid for 1 h and then with 1% OsO_4 for 2 h, dehydrated in ethanol series, and subjected to critical-point drying (HCP-2 critical point dryer, Hitachi) with dimethyl sulfoxide. After being mounted on brass studs with colloidal graphite with iso-propanol (Ted Pella, Redding, Calif.), the samples were ion-sputter-coated with Pt/Pd (E-1030, Hitachi) and observed under a Hitachi S-900 scanning electron microscope.

We examined toluidine-blue-stained sections at ×400 magnification for morphometric study and counted the numbers of hepatocytes and nonparenchymal cells that showed mitotic figures in ten microscopic fields (=0.84 mm^2). During mitosis, Kupffer cells and SECs were difficult to differentiate from one another by LM, so they were counted together as nonparenchymal cells. Four or five sections obtained from two or three livers were analysed at each time period after endotoxin administration, and the average density of cells (average number per 0.84 mm^2 of liver parenchyma) was calculated.

A quantitative analysis of endothelial fenestration in untreated rats and hepatectomized rats 1.5 h after administration of saline or endotoxin was performed. Eight to twelve rats were used for each group. Under SEM, the liver lobes possessing both portal tracts and central veins on the fractured surface were chosen; the portal tract was identified by the presence of abundant connective tissue, and the central vein was identified by the presence of a limited amount of connective tissue and numerous sinusoidal connections giving the appearance of perforated vein walls [38]. Eight different SECs situated in the intermediate position relative to the portal and central veins were chosen from each rat: 64–96 cells in total for each group. Between 107 and 717 (average 289.6±28.2) fenestrae were analysed for each rat, or a total of 1,882–4,276 fenestrae for each group. Pictures were taken at a magnification of ×10,000. The diameter and area of each fenestra were measured and recorded using a Kontron IBAS-1 Image

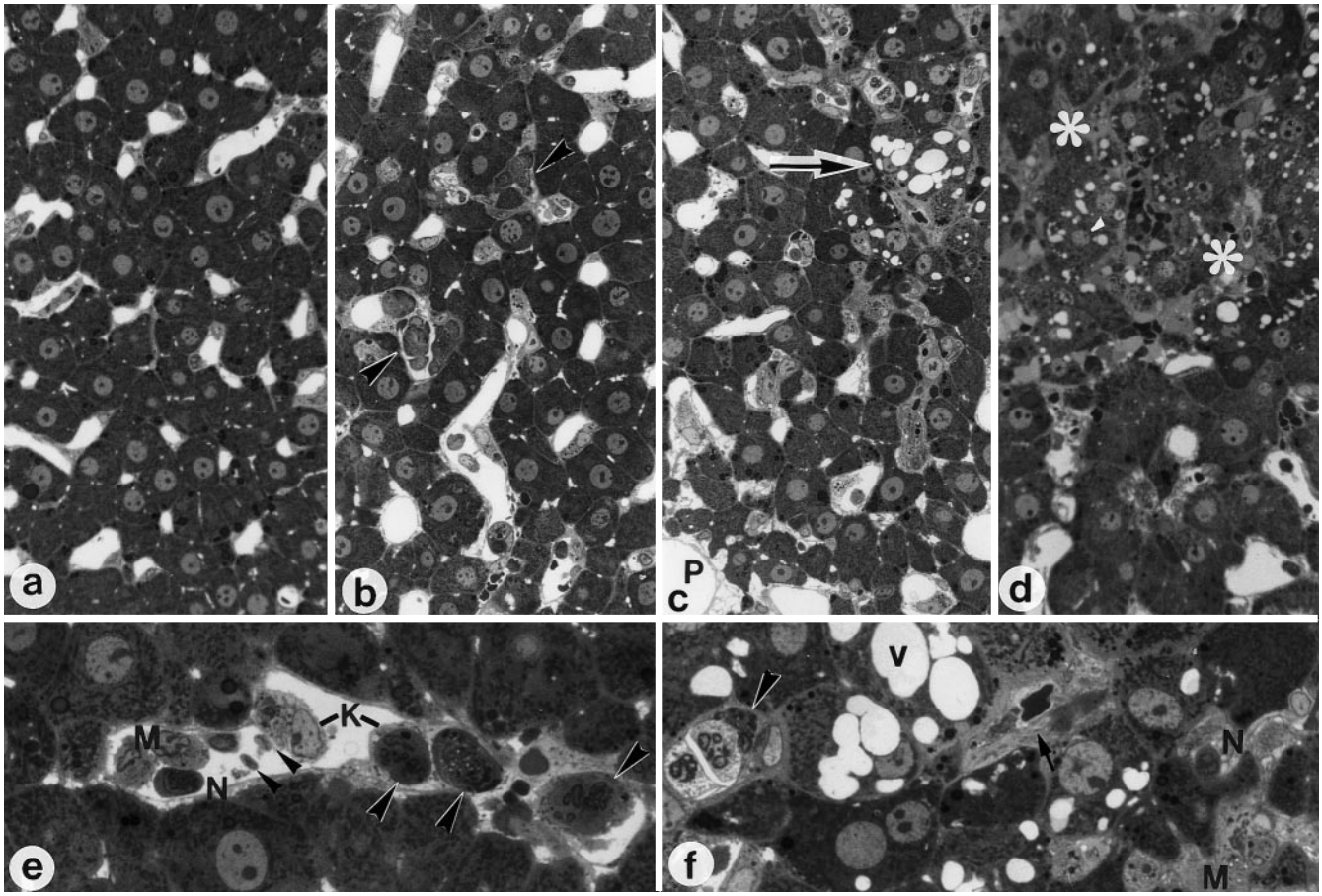

Fig. 2a–f Light micrographs of the livers from hepatectomized rats. Hepatectomy was performed 48 h before saline or endotoxin administration. **a** Immediately after endotoxin administration (Oh). **b**, **e** In the liver 1.5 h after endotoxin injection, neutrophils (*N*), monocytes (*M*) and platelets (*small arrowheads*) are apparent in the sinusoids, the neutrophils often being aggregated and phagocytosed by Kupffer cells (*K*), as indicated by *large arrowheads*. Some sinusoids in the midseptal region of intermediate or periportal zones are occluded by infiltrating leucocytes and swollen Kupffer cells. **c**, **f** At 3 h, some hepatocytes in the midseptal region exhibit vacuolation (*large arrow*). The sinusoids around vacuolated hepatocytes are occluded by neutrophils (*N*) and demonstrate neutrophil aggregation (*arrowhead*), macrophages (*M*) and fibrin deposits (*small arrow*). **d** At 5 h, hepatocytes demonstrate many blebs, which fill the space of Disse and sinusoids (*asterisks*; *P* portal veins, *v* vacuoles). Toluidine blue stain. **a–d** ×290, **e**, **f** ×720

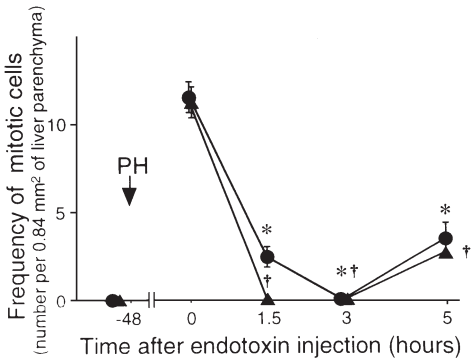

Fig. 3 Time course of mitosis of hepatocytes (-●-) and nonparenchymal cells (-▲-) as represented by the density of mitotic cells (no. per 0.84 mm^2 of liver parenchyma) after endotoxin administration. Partial hepatectomy (*PH*) was performed 48 h before endotoxin administration. Toluidine-blue-stained sections were observed at ×400. Ten microscopic fields were analysed for each section. Four to five sections from two or three animals were examined. Data are means±standard errors. *, †P<0.01 versus the value at 0 h

Analysis System (Kontron Bildanalyse, Munich, Germany). The average diameter and density of fenestrae and porosity of the sinusoidal walls (percentage of the total sinusoidal wall fenestrated) were then calculated.

All results were expressed as mean values±standard errors. The Mann-Whitney *U*-test and Wilcoxon's signed-rank test were used for the analysis of unpaired and paired samples, respectively.

Results

In this study, we used a rat model of liver failure induced by i.v. injection of low-dose endotoxin into hepatectomized rats 48 h after operation. While all 20 of the hepatectomized rats subjected to saline injection survived, 12 out of 20 (60%) hepatectomized rats given endotoxin died within 12 h, mostly 8–10 h, after the injection. To examine the pathogenesis of this experimental liver failure, the time-course of the morphological and functional alterations in SECs and hepatocytes were studied.

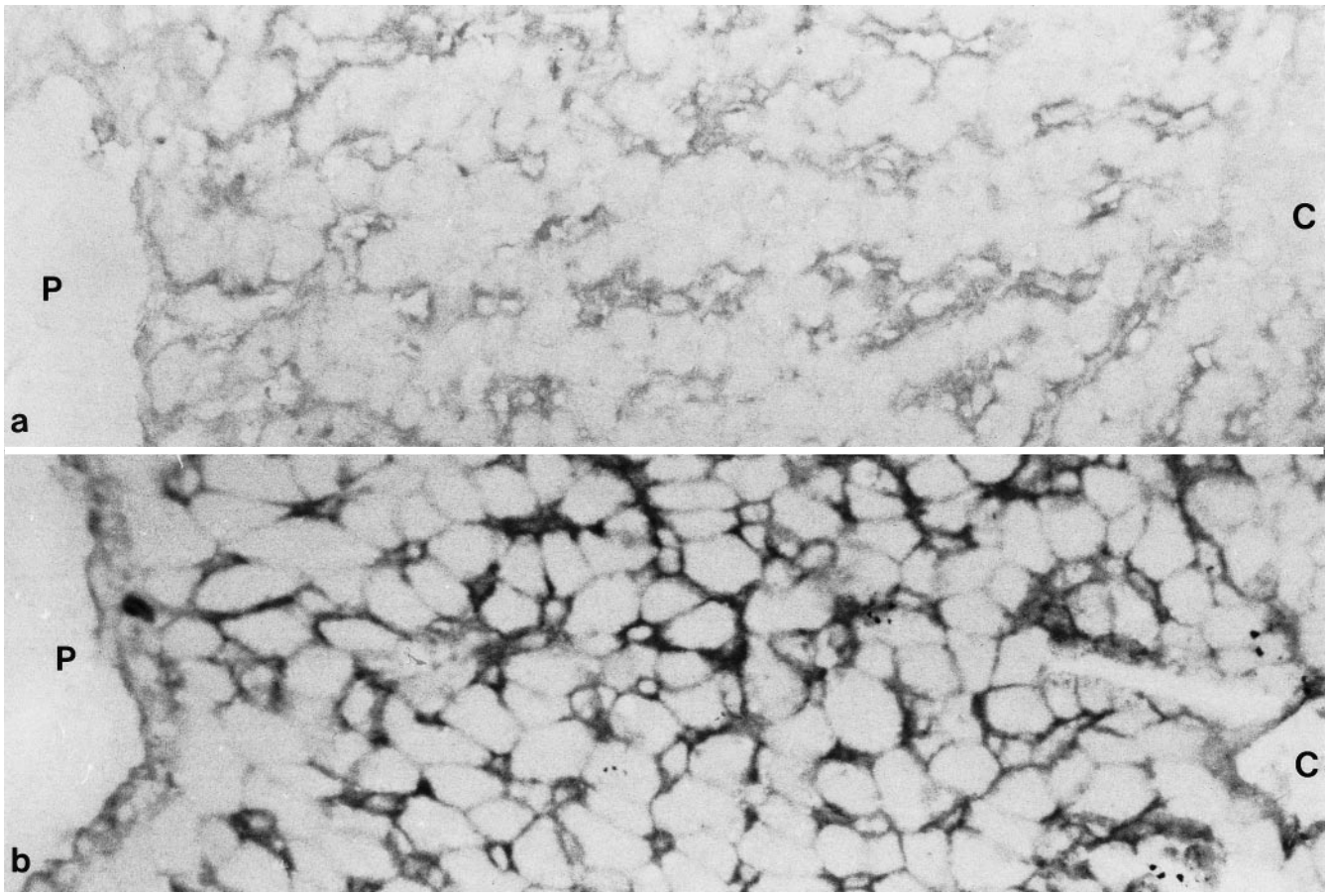

Fig. 4a, b Immunohistochemistry of the livers from hepatectomized rats for ICAM-1 expression. **a** Immediately after endotoxin administration (0 h). (**b**) At 1.5 h after endotoxin administration. Sinusoidal endothelial cells, vascular endothelial cells of portal veins (*P*) and central veins (*C*) are intensely stained for ICAM-1. LSAB-method, ×340

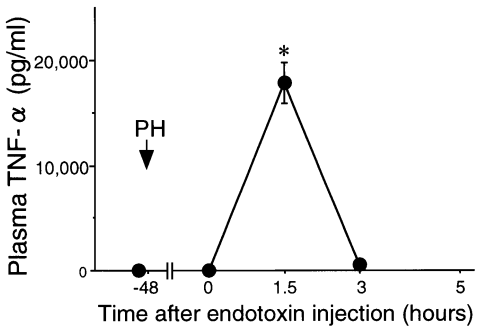

Fig. 5 Plasma TNF-α levels before partial hepatectomy (*PH*) and at various time points after endotoxin injection in hepatectomized rats. Hepatectomy was performed 48 h before endotoxin administration. Four rats were used for each time point. Data are means±standard errors. **P*<0.01 versus the value at 0 h

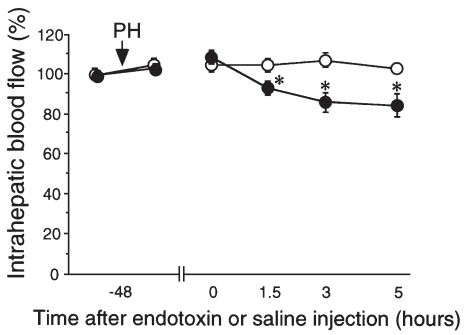

Fig. 6 Intrahepatic blood flow per unit square measured on the liver surface with a laser-Doppler flowmeter immediately before and after partial hepatectomy (*PH*) and at various time points after endotoxin (-●-) or saline (-○-) administration. Data are expressed as percentages of the values obtained before hepatectomy. Eight rats were examined at each time point. Data are means±standard errors. **P*<0.05 versus saline-treated rats at each time point

In the regenerating liver immediately after endotoxin administration there was no hepatocellular injury, as shown by normal serum levels of aminotransferases and total bilirubin (Fig. 1a, b) and normal LM features of hepatocytes (Fig. 2a). Both hepatocytes and nonparenchymal cells, including Kupffer cells and endothelial cells, frequently underwent mitosis (Fig. 3). There were no appreciable inflammatory changes such as leucocyte infiltration in the sinusoids (Fig. 2a). In agreement with this finding, ICAM-1 expression by SECs was only slight (Fig. 4a), and the plasma TNF-α level was not elevated (Fig. 5). The hepatic blood flow per unit square measured on the liver surface increased slightly (Fig. 6). The

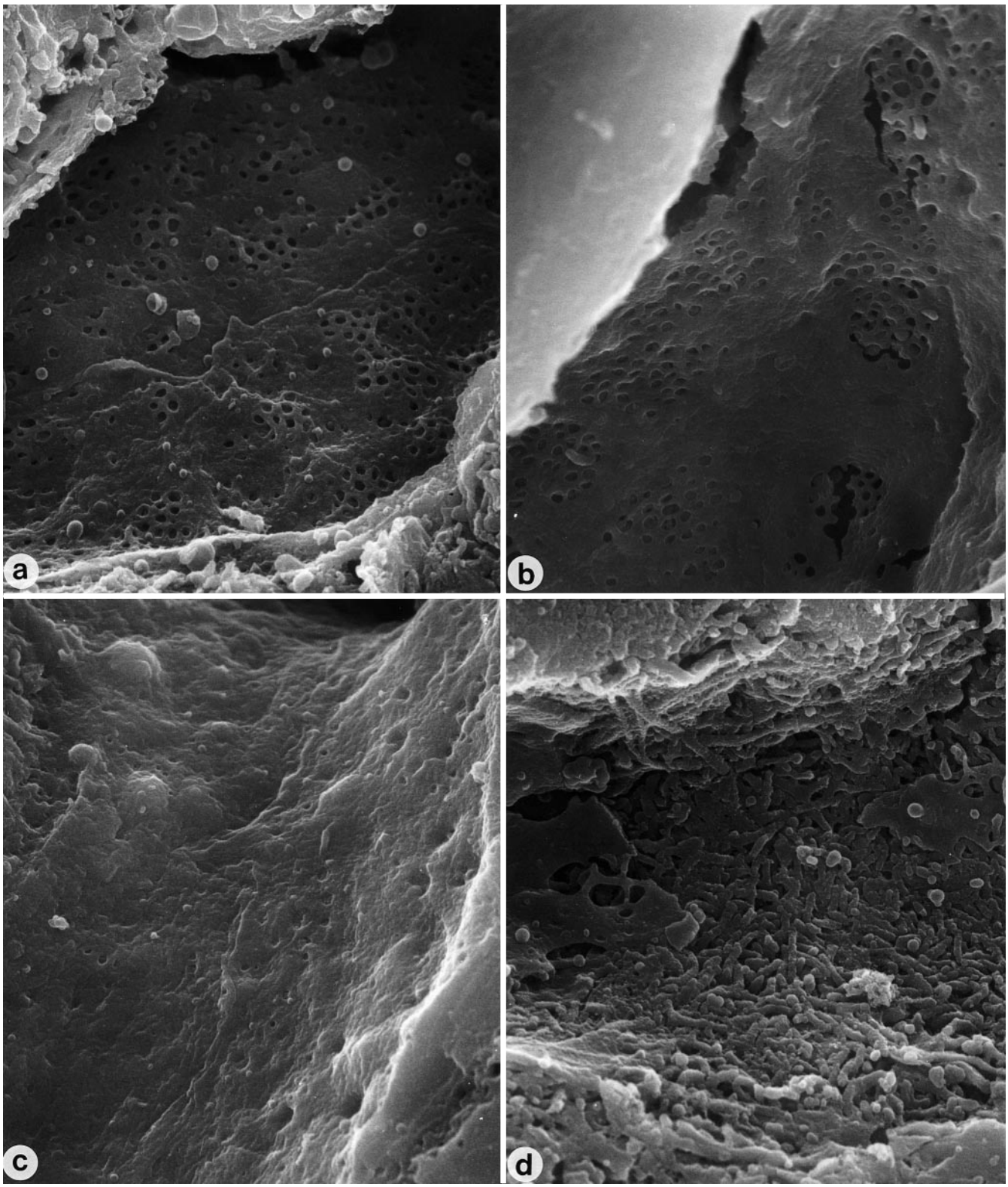

Fig. 7a–d Scanning electron micrographs of hepatic sinusoids in the intermediate zone of the liver lobule. **a** Nonhepatectomized liver. Sinusoidal endothelial cells show typical features of fenestration. **b** Hepatectomized rat liver immediately after endotoxin administration. The architecture of the sieve plates resembles that observed in **a**, although the frequency of fenestrae is decreased. **c** Hepatectomized rat liver 1.5 h after endotoxin administration. The characteristic sieve-plate pattern is lost, and the number of fenestrae is significantly reduced. **d** Hepatectomized rat liver 3 h after endotoxin administration. Endothelial cells are disrupted and detached in places, and hepatocellular microvilli are directly exposed to the sinusoidal lumen. **a**, **b** ×14,000, **c**, **d** ×13,000

Table 1 Diameter and density of endothelial fenestrae and porosity of sinusoidal walls in nonhepatectomized and hepatectomized rats 1.5 h after saline or endotoxin administration. Rats were subjected to an i.v. injection of saline or endotoxin 48 h after two-thirds partial hepatectomy, and 90 min after the injection their livers were analysed by scanning electron microscopy. We examined 4276, 1882 and 2168 fenestrae from the indicated numbers of nonhepatectomized and of saline-treated and endotoxin-treated hepatectomized rats, respectively. The values are means±standard errors

Treatments	No. of rats	Fenestrae		
		Diameter (nm)	Density (No./μm²)	Porosity (%)
Nonhepatectomized				
+ Saline	11	108.7±0.6	8.97±0.75	5.72±0.50
Hepatectomized				
+ Saline	8	105.4±1.0*	6.11±0.75*	3.66±0.44*
+ Endotoxin	12	100.2±1.0*,†	4.18±0.47*,†	2.14±0.21*,†

*P<0.01 versus nonhepatectomized rats; †P<0.01 versus saline-treated, hepatectomized rats

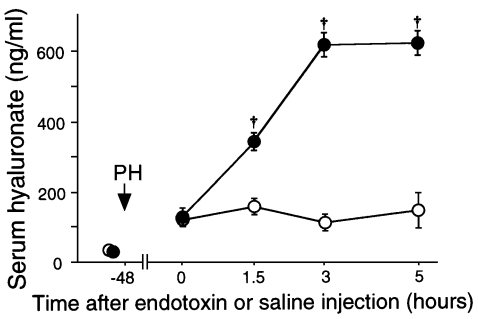

Fig. 8 Serum hyaluronate levels before partial hepatectomy (*PH*) and at various time points after i.v. injection of saline (-○-) or 200 μg/kg body weight of endotoxin (-●-). Hepatectomy was performed 48 h before saline or endotoxin administration. Elevation of serum hyaluronate levels is apparent at 1.5 h after endotoxin administration, preceding increase of alanine aminotransferase and total bilirubin. Eight rats were examined at each time point. Data are means±standard errors. †P<0.005 versus the value for saline-treated rats at each time point

SEM analysis demonstrated that, compared with normal features in nonhepatectomized rats (Fig. 7a), SECs in the hepatectomized rats had morphological modifications. Although the architecture of the sieve plates was well preserved, the number and diameter of fenestrae and porosity of the sinusoidal walls were significantly decreased (Fig. 7b, Table 1). The serum level of hyaluronate as a measure of the functional state of SECs showed a mild increase (Fig. 8).

At 1.5 h after endotoxin administration hepatocellular injury was not evident, as demonstrated by the absence of any significant elevation of serum aminotransferases and total bilirubin levels (Fig. 1a, b) and of degenerative features in hepatocytes on LM (Fig. 2b). Mitotic figures in hepatocytes decreased strikingly in frequency, and none at all were found in nonparenchymal cells (Fig. 3). There was marked infiltration of neutrophils and monocytes, particularly in the sinusoids of the midseptal regions of intermediate and periportal zones (Fig. 2b). Neutrophils, which were often aggregated in the sinusoids, were phagocytosed and digested by enlarged Kupffer cells (Fig. 2e). Platelets were also observed adhering to the sinusoidal wall (Fig. 2e). Transmigration of neutrophils and platelets into the space of Disse was also seen. The expression of ICAM-1 by SECs was profoundly augmented throughout the liver lobule (Fig. 4b), and the plasma TNF-α concentration increased considerably and reached a peak at an average value of 1.8×10^4 pg/ml (Fig. 5). The hepatic blood flow dropped by approximately 10% (Fig. 6). In SECs, the sieve-plate arrangement of fenestrations disappeared, and the frequency of fenestrae and porosity of the sinusoidal walls were significantly decreased at 1.5 h (Fig. 7c, Table 1). In TEM observations, SECs often exhibited acute swelling; the cell volume was increased and the cytoplasm became pale (Fig. 9a, c). Cellular hypertrophy was often accompanied by a moderate to high degree of increase in cell organelles such as vesicles, polysomes and dense bodies, indicative of SEC activation (Fig. 9b). While mitochondria sometimes exhibited degenerative signs (loss of matrix or vacuolation; Fig. 9c), most of the cell organelles had intact profiles. Neither Weibel-Palade bodies nor complete basement membranes characteristic of capillaries were found. There were no fibrin deposits along the sinusoidal lining cells. The serum hyaluronate level was significantly elevated to approximately 2.5-fold that at 0 h (Fig. 8).

At 3 h, serum transaminases and total bilirubin levels were significantly increased (Fig. 1a, b). On LM, the initial morphological evidence of hepatocellular degeneration (vacuolation) was found (Fig. 2c, f). Mitosis of hepatocytes and nonparenchymal cells remained entirely suppressed (Fig. 3). Leucocyte infiltration became more extensive in the midseptal region of intermediate and periportal zones (Fig. 2c). Fibrin deposits appeared along the sinusoidal walls (Fig. 2f). Plasma TNF-α levels returned to normal at this time point (Fig. 5). The hepatic blood flow dropped further to about 80% of the value measured at 0 h (Fig. 6). On SEM, the sieve plates of SECs were often seen to be disrupted, resulting in the direct exposure of hepatocellular microvilli to the sinusoidal lumen (Fig. 7d). Analysis by TEM demonstrated that SECs became necrotic in appearance, with their cytoplasm dissolved (Fig. 10a). Furthermore, SECs were dis-

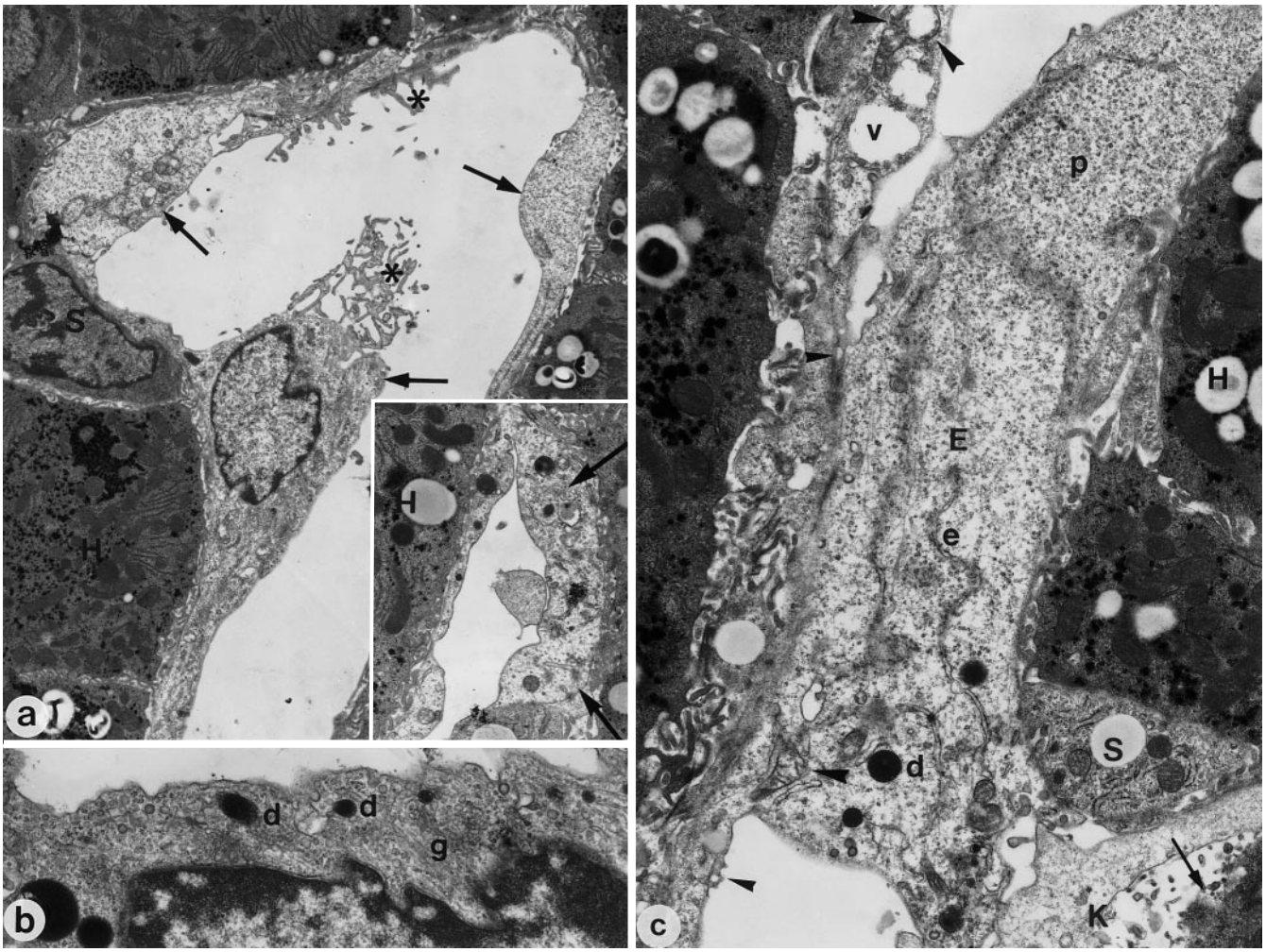

Fig. 9a–c Transmission electron micrographs of the livers from hepatectomized rats 1.5 h after endotoxin administration. Hepatectomy was performed 48 h before endotoxin injection. **a** Endothelial cells (*arrows*) are pale and swollen (*H* hepatocytes, *S* stellate cells, *asterisks* parts of Kupffer cells). **b** An endothelial cell enriched with cell organelles. It has several dense bodies (*d*), Golgi apparatuses (*g*) and vesicles at the luminal aspect of the nucleus and exhibits an undulating cell surface. **c** Swelling of endothelial cells (*E*) with rough endoplasmic reticulum (*e*) and dense bodies (*d*). A cluster of polysomes (*p*) is also seen. A small number of fenestrae (*small arrowheads*) is present. A part of endothelial cell is undergoing degeneration, as indicated by the occurrence of vacuoles (*v*). Some of the mitochondria (*large arrowheads*) are swollen and moderately vacuolated. Fibrin deposits, however, are not seen on the surface of endothelial cells. A Kupffer cell (*K*) nearby has a large phagosome (*arrow*; *H* hepatocytes, *S* stellate cells). **a** ×3,400, *inset* ×5,100, **b** ×9,200, **c** ×8,600

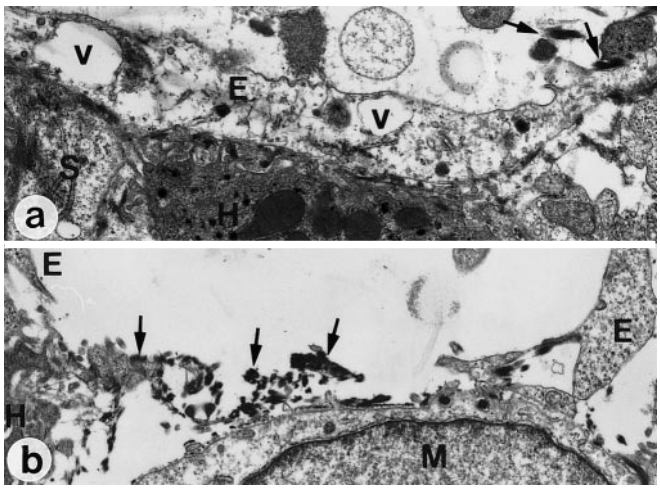

Fig. 10a, b Transmission electron micrographs of the livers from hepatectomized rats 3 h after endotoxin administration. Hepatectomy was performed 48 h before endotoxin injection. **a** Endothelial cells (*E*) are necrotic, with the cytoplasm dissolved out and mitochondria vacuolated (*v*). Fibrin deposits (*arrows*) are evident on the surfaces of endothelial cells (*H* hepatocytes, *S* stellate cells). **b** In some portions, endothelial cells (*E*) are disrupted with prominent fibrin deposits (*arrows*; *H* hepatocytes, *M* extrasinusoidally migrating macrophages). **a** ×6,500, **b** ×6,400

rupted, being accompanied by prominent fibrin deposits (Fig. 10b). The serum hyaluronate level showed a further increase (Fig. 8).

At 5 h, serum levels of transaminases and total bilirubin were considerably elevated (Fig. 1a, b). Hepatocytes underwent extensive degeneration (pale and swollen cytoplasm and generation of abundant blebs were seen, but there were no typical apoptotic bodies; Fig. 2d). The sinu-

soidal lumen was occupied by abundant infiltrating leucocytes and the blebs released from hepatocytes (Fig. 2d), and the hepatic blood flow was kept low (Fig. 6).

Discussion

In the rat model of liver failure, the serum hyaluronate level had risen significantly by 1.5 h after endotoxin administration, preceding the elevation of serum aminotransferases and bilirubin, suggesting that monitoring of this indicator may be useful in prediction of postoperative liver failure prior to clinical manifestation of liver injury, although hepatectomy itself elevates serum hyaluronate to some extent owing to decreased total hepatic flow via shunting of blood past the sinusoid [11, 15]. We have actually observed a significant increase in serum hyaluronate levels in all of 36 patients who underwent major hepatectomy (S. Yachida et al., unpublished data). In particular, those patients who developed postoperative hepatic failure showed a steep elevation in the early period after surgery.

The elevation of serum hyaluronate seen at 1.5 h strongly suggests functional perturbation of SECs [6, 7, 27, 31], although there might be some contribution of endotoxin-induced reduction of hepatic blood flow to this elevation. Morphological analyses demonstrated that SECs examined at this time point exhibited the features representative of SEC activation (they were swollen and enriched with cell organelles, and expressed ICAM-1 strongly). It is not probable that these features are related to SEC proliferation because mitosis of nonparenchymal cells was not found at this time point. Endothelial cell activation is generally seen in various tissues during acute inflammation: for example, in the skin TNF induces endothelial hypertrophy and augments the expression of adhesion molecules in vascular endothelial cells, resulting in intravascular accumulation of leucocytes [21]. In the liver, TNF-α elicits hepatic microvascular responses such as leucocyte adhesion to SECs and swelling of SECs, leading to narrowing of the sinusoidal lumen and impairment of sinusoidal blood flow [17, 18]. We observed here a prominent elevation of plasma TNF-α levels at 1.5 h, as previously reported [30]. TNF-α is a primary mediator of endotoxic events [33], and endothelial cells activated by TNF-α release interleukin (IL)-8, which promotes neutrophil transmigration [3]; it seems, then, that the inflammatory reactions of sinusoids seen here (endothelial swelling, intrasinusoidal infiltration and transluminal migration of leucocytes) are most probably mediated by TNF-α. Apart from TNF-α, various cytokines, such as IL-1 and IL-6, or vasoactive substances, such as nitric oxide and endothelin, are induced by endotoxin administration; they may also be involved in the modulation of inflammatory reactions [16, 23, 29]. Defenestration of SECs, as observed by SEM at 1.5 h, may be also a feature relevant to cytokine-induced activation of SECs, because cytokines such as TNF-α and leukotrienes released from endotoxin-activated Kupffer cells mediate endothelial defenestration [26] by rearrangement of the cytoskeleton [28]. These cytokines and leukotrienes have been also shown to suppress hyaluronate scavenging [7, 8]. It is reported that, in capillarized sinusoids, SECs show reduced binding and degradation of hyaluronate by decrease of hyaluronate receptors, resulting in an elevation of serum hyaluronate [31, 34]. The present study has demonstrated that sinusoidal defenestration induced by acute inflammatory reactions is similarly associated with the elevation of serum hyaluronate.

The necrosis and disruption of SECs, together with fibrin deposits, observed following SEC activation have also been reported in rats treated with *Propionibacterium acnes*/endotoxin and considered to be attributable to the toxic effects of superoxide and TNF-α released from endotoxin-activated Kupffer cells [1, 39]. Neutrophils primed by TNF-α may be also responsible for production of superoxide anions [30]. Furthermore, TNF-α enhances the susceptibility of vascular endothelial cells to neutrophil-mediated attack [35]. In the present study, prominent infiltration of neutrophils was observed in the sinusoids of hepatectomized rats 1.5 h after endotoxin administration, which is consistent with a previous report [30]. Taking these data into account, the features of SEC activation at 1.5 h and SEC injury at 3 h may reflect two different stages of sequential changes induced by cytokines and superoxide anions released from endotoxin-activated Kupffer cells. Pober [25] has noted that distinction of endothelial cell activation from injury or dysfunction is complex, because activation can produce dysfunction with or without injury.

In the present study, hepatic necrosis preferentially occurred in the “midseptal region” [9] of the intermediate and periportal zones, in which sinusoidal blood flow is considered to be lower than in other regions [40], suggesting that in addition to toxic effects of TNF-α and superoxide, the impairment of hepatic blood flow induced by both local and systemic effects of endotoxin may be important for the development of hepatic necrosis. Hepatic stellate cells, or pericytes of sinusoids, will subsequently be activated in the post-necrotic region and involved in the pathogenesis of acute liver failure [12].

In conclusion, SECs undergo morphological and functional alterations representative of cellular activation as their earliest inflammatory response. This is followed by degenerative changes of SECs and hepatocytes in endotoxin-induced liver failure after partial hepatectomy.

Acknowledgements We thank Miss Makimi Ishii, First Department of Surgery, and Mr. Hiroshi Miyanaka, Research Equipment Center, Kagawa Medical University, for the valuable technical assistance with the scanning electron microscopy.

References

1. Arai M, Mochida S, Ohno A, Ogata I, Fujiwara K (1993) Sinusoidal endothelial cell damage by activated macrophages in rat liver necrosis. Gastroenterology 104:1466–1471
2. Arvidsson D, Svensson H, Haglund U (1988) Laser-Doppler flowmetry for estimating liver blood flow. Am J Physiol 254:G471-G476

3. Baggiolini M, Walz A, Kunkel SL (1989) Neutrophil-activating peptide-1/interleukin 8, a novel cytokine that activates neutrophils. J Clin Invest 84:1045–1049
4. Boermeester MA, Straatsburg IH, Houdijk APJ, Meyer C, Frederiks WM, Wesdorp RIC, Van Noorden CJF, Van Leeuwen PAM (1995) Endotoxin and interleukin-1 related hepatic inflammatory response promotes liver failure after partial hepatectomy. Hepatology 22:1499–1506
5. Chichibu K, Matsuura T, Shichijo S, Yokoyama MM (1989) Assay of serum hyaluronic acid in clinical application. Clin Chim Acta 181:317–324
6. Deaciuc IV, Bagby GJ, Lang CH, Spitzer JJ (1993) Hyaluronic acid uptake by the isolated, perfused rat liver: an index of hepatic sinusoidal endothelial cell function. Hepatology 17:266–272
7. Deaciuc IV, Bagby GJ, Lang CH, Skrepnik N, Spitzer JJ (1993) Gram-negative bacterial lipopolysaccharide impairs hyaluronan clearance in vivo and its uptake by the isolated, perfused rat liver. Hepatology 18:173–178
8. Deaciuc IV, Bagby GJ, Niesman MR, Skrepnik N, Spitzer JJ (1994) Modulation of hepatic sinusoidal endothelial cell function by Kupffer cells: an example of intercellular communication in the liver. Hepatology 19:464–470
9. Ekataksin W, Wake K (1991) Liver units in three dimensions. I. Organization of argyrophilic connective tissue skeleton in porcine liver with particular reference to the “compound hepatic lobule.” Am J Anat 191:113–153
10. Fujiwara K, Ogata I, Mochida S, Yamada S, Hirata K, Tomiya T, Ohta Y (1990) Activated Kupffer cells as a factor of massive hepatic necrosis after liver resection. Hepatogastroenterology 37:194–197
11. Gibson PR, Fraser JRE, Brown TJ, Finch CF, Jones PA, Colman JC, Dudley FJ (1992) Hemodynamic and liver function predictors of serum hyaluronan in alcoholic liver disease. Hepatology 15:1054–1059
12. Hautekeete ML, Geerts A (1997) The hepatic stellate (Ito) cell: its role in human liver disease. Virchows Arch 430:195–207
13. Higgins GM, Anderson RM (1931) Experimental pathology of the liver. I. Restoration of the liver of the white rat following partial surgical removal. Arch Pathol 12:186–202
14. Laurent TC, Fraser JRE (1992) Hyaluronan. FASEB J 6:2397–2404
15. Lebel L, Fraser JRE, Kimpton WS, Gabrielsson J, Gerdin B, Laurent TC (1989) A pharmacokinetic model of intravenously administered hyaluronan in sheep. Pharm Res 6:677–682
16. Luster MI, Germolec DR, Yoshida T, Kayama F, Thompson M (1994) Endotoxin-induced cytokine gene expression and excretion in the liver. Hepatology 19:480–488
17. McCuskey RS (1994) The hepatic microvascular system. In: Arias IM, Boyer JL, Fausto N, Jakoby WB, Schachter DA, Schafritz DA (eds) The liver: biology and pathobiology, 3rd edn. Raven Press, New York, pp 1089–1106
18. McCuskey RS, Urbaschek R, McCuskey PA, Urbashek B (1989) Hepatic microvascular responses to tumor necrosis factor. In: Wisse E, Knook DL, Decker K (eds) Cells of the hepatic sinusoid, vol 2. The Kupffer Cell Foundation, Rijswijk, pp 272–276
19. Mizock BA (1985) Branched-chain amino acids in sepsis and hepatic failure. Arch Intern Med 145:1284–1288
20. Mochida S, Ogata I, Hirata K, Ohta Y, Yamada S, Fujiwara K (1990) Provocation of massive hepatic necrosis by endotoxin after partial hepatectomy in rats. Gastroenterology 99:771–777
21. Munro JM, Pober JS, Cotran RS (1989) Tumor necrosis factor and interferon-γ induce distinct patterns of endothelial activation and associated leukocyte accumulation in skin of *Papio anubis*. Am J Pathol 135:121–133
22. Nadig DE, Wade TP, Fairchild RB, Virgo KS, Johnson FE (1997) Major hepatic resection: indications and results in a national hospital system from 1988 to 1992. Arch Surg 132:115–119
23. Nishida J, Fox ES, McDonnell D, Baker GL, Ekataksin W, McCuskey RS (1995) Role of nitric oxide in the interaction of leukocytes with hepatic sinusoidal lining cells during endotoxemia. In: Wisse E, Knook DL, Wake K (eds) Cells of the hepatic sinusoid, vol 5. The Kupffer Cell Foundation, Leiden, pp 270–271
24. Okano K, Kokudo Y, Okajima K, Hossain MA, Ishimura K, Yachida S, Tsubouchi T, Wakabayashi H, Maeba T, Maeta H (1996) Protective effects of antithrombin III supplementation on warm ischemia and reperfusion injury in rat liver. World J Surg 20:1069–1075
25. Pober JS (1988) Cytokine-mediated activation of vascular endothelium: physiology and pathology. Am J Pathol 133:426–433
26. Sarphie TG, D’Souza NB, Deaciuc IV (1996) Kupffer cell inactivation prevents lipopolysaccharide-induced structural changes in the rat liver sinusoid: an electron-microscopic study. Hepatology 23:788–796
27. Shimizu H, He W, Guo P, Dziadkoviec I, Miyazaki M, Falk RE (1994) Serum hyaluronate in the assessment of liver endothelial cell function after orthotopic liver transplantation in the rat. Hepatology 20:1323–1329
28. Stolpen AH, Guinan EC, Fiers W, Pober JS (1986) Recombinant tumor necrosis factor and immune interferon act singly and in combination to reorganize human vascular endothelial cell monolayers. Am J Pathol 123:16–24
29. Sugiura M, Inagami T, Kon V (1989) Endotoxin stimulates endothelin-release in vivo and in vitro as determined by radioimmunoassay. Biochem Biophys Res Commun 161:1220–1227
30. Suzuki S, Nakamura S, Serizawa A, Sakaguchi T, Konno H, Muro H, Kosugi I, Baba S (1996) Role of Kupffer cells and the spleen in modulation of endotoxin-induced liver injury after partial hepatectomy. Hepatology 24:219–225
31. Tamaki S, Ueno T, Torimura T, Sata M, Tanikawa K (1996) Evaluation of hyaluronic acid binding ability of hepatic sinusoidal endothelial cells in rats with liver cirrhosis. Gastroenterology 111:1049–1057
32. Tamatani T, Miyasaka M (1990) Identification of monoclonal antibodies reactive with the rat homolog of ICAM-1, and evidence for a differential involvement of ICAM-1 in the adherence of resting versus activated lymphocytes to high endothelial cells. Int Immunol 2:165–171
33. Tracey KJ, Beutler B, Lowry SF, Merryweather J, Wolpe S, Milsark IW, Hariri RJ, Fahey TJ III, Zentella A, Albert JD, Shires GT, Cerami A (1986) Shock and tissue injury induced by recombinant human cachectin. Science 234:470–474
34. Ueno T, Inuzuka S, Torimura T, Tamaki S, Koh H, Kin M, Minetoma T, Kimura Y, Ohira H, Sata M, Yoshida H, Tanikawa K (1993) Serum hyaluronate reflects hepatic sinusoidal capillarization. Gastroenterology 105:475–481
35. Varani J, Bendelow MJ, Sealey DE, Kunkel SL, Gannon DE, Ryan US, Ward PA (1988) Tumor necrosis factor enhances susceptibility of vascular endothelial cells to neutrophil-mediated killing. Lab Invest 59:292–295
36. Wang XD, Andersson R, Soltesz V, Bengmark S (1992) Bacterial translocation after major hepatectomy in patients and rats. Arch Surg 127:1101–1106
37. Wang XD, Pärsson H, Andersson R, Soltesz V, Johansson K, Bengmark S (1994) Bacterial translocation, intestinal ultrastructure and cell membrane permeability early after major liver resection in the rat. Br J Surg 81:579–584
38. Wisse E, De Zanger RB, Van Der Smissen P, McCuskey RS (1985) The liver sieve: considerations concerning the structure and function of endothelial fenestrae, the sinusoidal wall and the space of Disse. Hapatology 5:683–692
39. Yamada S, Ogata I, Hirata K, Mochida S, Tomiya T, Fujiwara K (1989) Intravascular coagulation in the development of massive hepatic necrosis induced by *Corynebacterium parvum* and endotoxin in rats. Scand J Gastroenterol 24:293–298
40. Zou Z, Ekataksin W, Wake K (1998) Zonal and regional differences identified from precision of vitamin A-storing lipid droplets of the hepatic stellate cells in pig liver: a novel concept of addressing the intralobular area of heterogeneity. Hepatology 27:1098–1109